An optical lattice clock based on bosonic Sr

Nicola Poli, Marco G. Tarallo, Marco Schioppo, Christopher W. Oates and Guglielmo M. Tino
Dipartimento di Fisica and LENS, Università di Firenze, INFN-Sezione di Firenze,
Via Sansone,1 - 50019 Sesto Fiorentino - Italia

***Abstract*— We present experimental results for an optical lattice clock operating on the $^1S_0 \leftrightarrow {}^3P_0$ transition in ^{88}Sr, which is excited with the technique of magnetic field-induced spectroscopy. To reduce the complexity of the setup we have developed a set of new experimental techniques that greatly simplifies the clock spectroscopy in Sr atoms. First, we developed a method for finding the clock transition that removes the need for extensive frequency metrology hardware and optical frequency combs. This technique exploits a near coincidence in the atomic wavelengths of the $^1S_0 \leftrightarrow {}^3P_0$ clock and $^1S_0 \leftrightarrow {}^3P_1$ second stage cooling transitions in Sr, which are only 5 THz far apart. This coincidence enables the use of an optical (transfer) cavity to reference the frequency of the clock transition relative to that of the much stronger cooling transition. Second, all laser sources in the experimental setup are based on semiconductor technology, which greatly reduces the complexity of the apparatus. With this setup, about 10^4 ^{88}Sr atoms are trapped in a 1D lattice formed by 200 mW of radiation tuned near the magic wavelength at 813 nm. Preliminar uncertainty budget for our optical lattice clock is also presented,with particular attention to density dependent collisions, which led to an unexpectedly high signal contrast for long interaction times.**

PACS: 06.30.Ft 42.62.Fi 32.70.Jz 37.10.Jk
42.62.Eh 42.55.Px

I. Introduction

Optical atomic clocks have recently reached levels of performance that are an order of magnitude or more beyond those of their microwave counterparts, which have historically set the standards for precision time/frequency metrology. With this improved level of precision, scientists are performing new and more stringent tests of fundamental physical principles such as relativity and searches for temporal drifts in the fundament constants [1], [2]. Additionally, we anticipate that many new applications will arise, including improved timing for space travel and accelerator centers, as well as perhaps a new type of relativity-based geodesy [3]. These applications will require more compact, robust, and versatile versions of optical atomic clocks. Thus far, state-of-the-art optical clocks, whether based on neutral or charged atoms, tend to be fairly complicated pieces of scientific apparatus. They usually require multiple (often sophisticated and power hungry) laser systems, operate in well controlled environmental conditions, and rely on links to well developed frequency standards. For these reasons, most optical clocks are being developed in or near metrology institutes.

Here we present a considerably simplified version of one of the most promising optical clock systems, the Sr lattice clock. Due to the favorable laser wavelengths required for its operation, the Sr lattice clock is a good choice for streamlining, and in fact is the most mature of lattice clocks, with many under development around the world [4]–[6], [8], [9]. In a recent demonstration, a Sr lattice clock achieved an absolute fractional frequency uncertainty (for ^{87}Sr) of 1.5 x 10^{-16} and a fractional instability of 10^{-16} for an averaging time of 200 s [6]. In our version of a ^{88}Sr lattice clock, we demonstrate two important simplifications [7]. First, we use only lasers that are based on semiconductor laser technology. These lasers considerably simplify the apparatus and greatly reduce the power/size requirements. Second, we take advantage of a coincidence in the Sr atomic energy level system to greatly simplify the needle-in-a-haystack challenge of locating the ultranarrow spectroscopic feature used for stabilizing the clock laser. This transfer cavity-based technique removes the need for support from a standards institute or a GPS-referenced femtosecond-laser frequency comb to calibrate the clock laser, and can correct unexpected length changes in the clock reference cavity (e.g., in a transportable device with a poorly controlled environment). This simplified search method is further aided by a new search algorithm based on chirping the laser frequency over a one-second probe period, which has led to spectroscopic features with a contrast greater than 99 %. These developments represent important steps towards a transportable device, which could enable long-distance frequency comparisons at well below the 10^{-15} level, and could also lead to simpler laboratory-based devices.

II. Diode laser-based Sr lattice clock apparatus

As pointed out in the introduction, the level scheme of neutral Sr offers some interesting advantages relative to other atoms/ions when realizing a compact optical atomic clock. All of the relevant transition wavelengths for cooling and trapping lie in the visible or near infrared and can be easily reached with semiconductor devices (see Fig.1). Further reduction of the complexity of the setup comes from the use of a magnetic-field-induced spectroscopy scheme to observe the doubly-forbidden $^1S_0 \leftrightarrow {}^3P_0$ clock transition on bosonic isotopes [10]–[12]. In this technique a static magnetic field is used to mix the 3P0 metastable state with the 3P1 state, enabling direct optical excitation of the clock transition with tunable transition rates. Details on our experimental setup and the laser sources used for cooling and trapping ^{88}Sr have been previously reported in [13], [14]. In brief, ^{88}Sr atoms are collected from a slowed Sr beam and cooled in a two-stage magneto-optical trap (MOT). The MOT uses the strong dipole allowed $^1S_0 \leftrightarrow {}^1P_1$ transition at 461 nm to cool and collect atoms, and then uses the intercombination $^1S_0 \leftrightarrow {}^3P_1$ transition at 689 nm to cool

978-1-4244-3510-4/09/$25.00 ©2009 IEEE

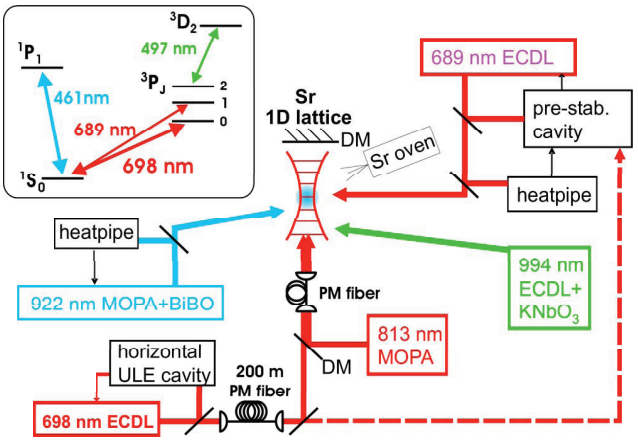

Fig. 1. Schematic of the Sr lattice clock apparatus. ECDL - external cavity diode laser, MOPA - optical amplifiers that are injection-locked by master lasers, DM - dichroic mirror. Inset: relevant atomic levels and optical transitions for the Sr lattice clock. All of the transitions are in the visible or in the near infrared and can be reached with semiconductor laser sources.

the atoms to a temperature of 1 μK. To generate the 461 nm light we double the frequency of a 922 nm diode/amplifier laser combination with a resonant cavity containing a bismuth triborate (BiBO) non-linear crystal. The second-stage cooling uses light from a frequency-stabilized 689 nm diode laser that is locked to a narrow resonance of a high-finesse Fabry-Perot cavity. The frequencies of the trapping lasers are stabilized to their respective atomic resonances by means of spectroscopy in Sr heat-pipes. To increase the first-stage MOT lifetime (and thus, the number of trapped atoms) repump light at 497 nm is used to keep the atoms from getting shelved in the $^3P_2$ state by exciting the $^3P_2 \leftrightarrow {}^3D_2$ transition. The 497 nm light is generated by doubling the frequency of a 994 nm diode laser with a resonant cavity containing a $KNbO_3$ crystal. To further simplify the apparatus, this doubled laser system at 497 nm could be replaced with two semiconductor lasers at 707 nm and 679 nm.

With this apparatus, typically 10^6 atoms are trapped at 1 μK in a loading period of 300 ms. About 10^5 atoms are then loaded into a 1D standing wave optical lattice operating at the magic wavelength for the $^1S_0 \leftrightarrow {}^3P_0$ clock transition (813.43 nm) [5]. A lattice potential depth of about 8 μK (or 50 E_r in units of the atomic recoil energy, E_r) is realized by tightly focusing (waist $\sim$ 30 μm) 200 mW of light coming from a 813 nm diode laser/amplifier combination. To prevent optical feedback in the tapered amplifier, which can induce phase fluctuations in the lattice potential that lead to atom loss, two 40 dB stages of optical isolation are necessary between the amplifier output and the atoms. Under these conditions the measured lifetime in our trap is around 2.5 s, limited by background gas collisions.

After the loading sequence, the $^1S_0 \leftrightarrow {}^3P_0$ clock transition at 698 nm is probed after a 50 ms delay that allows for the quadrupole magnetic MOT field to dissipate and the static magnetic field to be turned on for the spectroscopy. To reduce systematic effects related to the alignment of the probe with respect to the infrared laser, the probe and lattice beams are superimposed on a dichroic mirror and then coupled to the same single-mode optical fiber that delivers the light to the atom trap. After passing through the fiber, the two beams share the same polarization optics that define a linear polarization aligned with the vertical static magnetic field and the same achromatic lens that focuses light on the atomic cloud.

The red clock laser light is produced in a separate quiet room by frequency stabilization of a 698 nm extended cavity diode laser (ECDL) to high finesse resonant cavities [13]. Two steps of Pound-Drever-Hall frequency stabilization are employed to reduce the emission linewidth of the clock laser down to Hz level: first, we lock the laser frequency to a resonance of a pre-stabilization cavity (invar spacer, cavity finesse 10^4 with PZT), and then we lock the pre-stabilized laser to a resonance of a high finesse cavity (horizontal symmetric ULE cavity with finesse $4 * 10^5$) [15]. The combination of a 10 cm-long ULE spacer and fused silica mirrors for this cavity yields a thermal noise limited frequency instability of about $6{*}10^{-16}$. The ULE cavity is held under vacuum ($< 10^{-7}$ Torr) in a temperature-stabilized 50-mm thick aluminum can. Due to the particular choice of the material the CTE coefficient at 25 °C is $5{*}10^{-8}$ K. For vacuum-can thermal fluctuations of about 10 mK, the resulting frequency drift of the stabilized laser is typically 1 Hz/s. We have tested the frequency stability of the 698 nm clock source through comparison with a second ULE high finesse cavity. The measured Allan variance of the optical beatnote between two beams independently locked to the two cavities showed a frequency instability of $2{*}10^{-15}$ at 100 s, mainly limited by residual noise in the servo electronics and uncompensated frequency drifts [16].

To find the 698 nm transition for the first time, we took advantage of the comparatively small difference in wavelength between the second-stage cooling laser (689 nm) and the clock laser (698 nm) in Sr. In this way, it is then possible to calibrate a commercial wavemeter by using the 689 nm light, which is locked to the well-known frequency of the $^1S_0 \leftrightarrow {}^3P_1$ transition [18], [19], and perform and absolute uncertainty for the 698 nm clock laser frequency of less than 5 MHz.

While this method provides an uncertainty level low enough to find the clock transition in a few trials (see next section), it is also possible to remove the need for the wavemeter on a day-to-day basis altogether, through use of the 689 nm pre-stabilization cavity as a transfer cavity [20], [21].

Moreover, for the first research of the transition on daily basis it is possible to apply a fast frequency chirping to the clock light frequency (with a typical rate of 100 kHz/s). We could then scan over a large interval of frequency values in a short period, which greatly accelerated initial searches for the clock transition, as we will describe. The atoms left in the ground state after the spectroscopy pulse are detected and counted by detecting the fluorescence induced by a 461 nm resonant probe beam.

This method finds application not only in lab-based experiments, but also in future transportable devices, where frequent

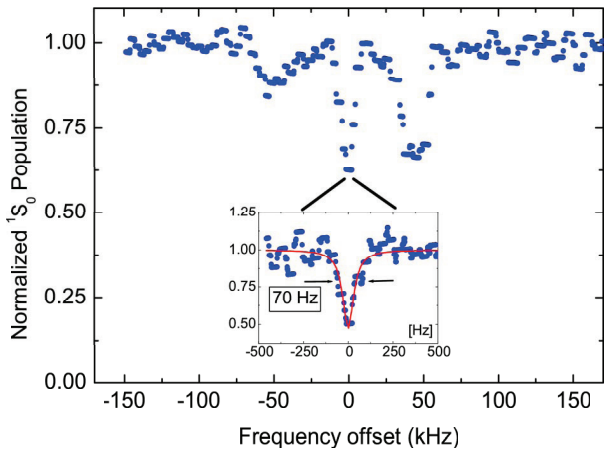

Fig. 2. High resolution spectrum of the $^1S_0 \leftrightarrow {}^3P_0$ transition taken by scanning the probe laser frequency (without chirping). The spectrum is obtained with a static magnetic field B_0 = 13 mT and probe intensity I=38 W/cm^2 with an interaction period τ = 100 ms. The separation between the carrier and the two sidebands (Δ = 50 kHz) indicates a lattice depth of 55 E_r. In the inset is shown a scan of the carrier with B_0 = 1.3 mT, I = 6 W/cm^2 and the same interaction period. The observed 70 Hz linewidth is limited by the induced Rabi frequency in this condition (see text). For both spectra the lattice wavelength has been tuned near the magic wavelength at 813.428 nm

calibrations (e.g., due to shocks on reference cavities) could be necessary, and where the access to frequency combs and frequency references could be limited. By using the cavity transfer method, even when shocks change the mode numbers considerably, a few trials with different modes of the transfer cavity could be sufficient to reset the offset between the transfer cavity and the probe laser reference cavity without the need of external references.

III. Spectroscopy of the Clock Transition

We excite the $^1S_0 \leftrightarrow {}^3P_0$ clock transition in ^{88}Sr with the technique of magnetic field-induced spectroscopy [10]. We initially find the transition by chirping the probe laser frequency over 200 kHz during each 1 s probe pulse in order to increase the searching rate. With a maximum magnetic field of 16 mT and a probe light intensity of 40 W/cm^2, the effective Rabi frequency is estimated to be 13 kHz. This frequency is sufficiently high to ensure observable population transfer on resonance within the chirp range. Under these conditions we can find the transition quickly by taking 200 kHz frequency steps around the resonance and measuring the ground state population. We prove this search method to be effective even in the case of a poor knowledge of the probe frequency, calibrated only using a commercial wavemeter.

In Fig. 2 the data were taken without frequency chirping and with a reduced interaction time of 100 ms. The two spectra have been taken with static magnetic fields (B_0) of 13 mT and 1.3 mT (for the spectrum in the inset) respectively, and the probe intensities (I) were 38 W/cm^2 and 6 W/cm^2 (for the inset), giving induced Rabi frequencies (Ω) of 10 kHz and 130 Hz (inset). Higher-resolution spectra are shown in Fig. 2). From the frequency spacing and the amplitude ratio between the red and blue sidebands signals, we determined a lattice depth of U_0 = 55 E$_r$ and an estimated temperature of 2.6 μK.

IV. Inelastic Collisions between Atoms in Ground 1S0 and Excited 3P0 State

We examined the decay of the ground state population for overdriven Rabi excitation (see Fig. 3) and compared it to the lifetime of the trap in the absence of resonant excitation on clock transition. From the decay plots, it is clear that when resonant clock light is present, the atoms are lost at a higher rate compared to the normal decay rate that results from background gas collisions that limit the trap lifetime to about $\tau = 1/\Gamma$=3 s. The faster decay in the presence of excitation light can be well described by the solution to a system of coupled rate equations $\dot{n}_S = -\Gamma n_S - \Omega(n_S - n_P) - w\, n_S n_P$, $\dot{n}_P = -\Gamma n_P - \beta n_P^2 + \Omega(n_S - n_P) - w\, n_S n_P$ [22]. These equations describe the evolution of density of atoms n_S in the ^{1}S$_0$ ground state and n_P for the excited ^{3}P$_0$ state, respectively. In these two equations we introduce additional density-dependent loss terms β and w associated with density-dependent losses due to collisions between atom pairs in the excited state and collisions between ground- and excited-state atoms, respectively. The atomic density in the ground state is estimated from the measurement of the trap frequencies and atom temperature with an uncertainty of 50 %. Assuming a value of β = 4*10^{-18} m^3/s [23] from the fit of the experimental data with the solution of the decay equations, we estimate the value for interstate collision coefficient to be w = 3(2)*10^{-17} m^3/s at measurement temperature of

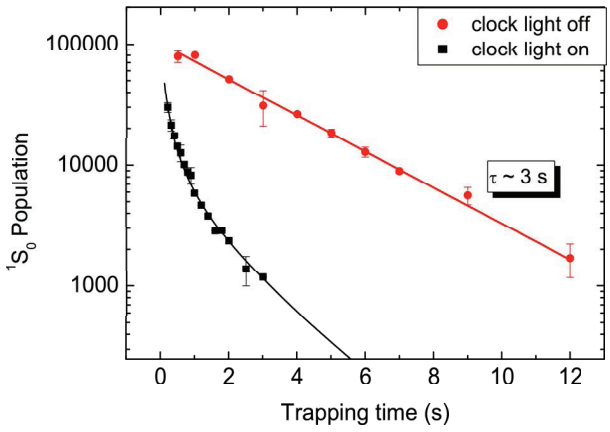

Fig. 3. Comparison of ground-state population decays. Data in circles represent the lifetime of the 813 nm lattice trap and fit well to a single exponential (solid line), vacuum limited to 2.9 s. The second, faster, decay is measured in the presence of the clock light tuned to the carrier resonance at 698 nm. These data agree well with a model based on a system of coupled rate equations (see text) indicated by the solid (lower) line. The non-exponential fast decay indicates an additional density-dependent loss mechanism due to collisions of atoms in the ^{3}P$_0$ upper state with atoms in the ground state.

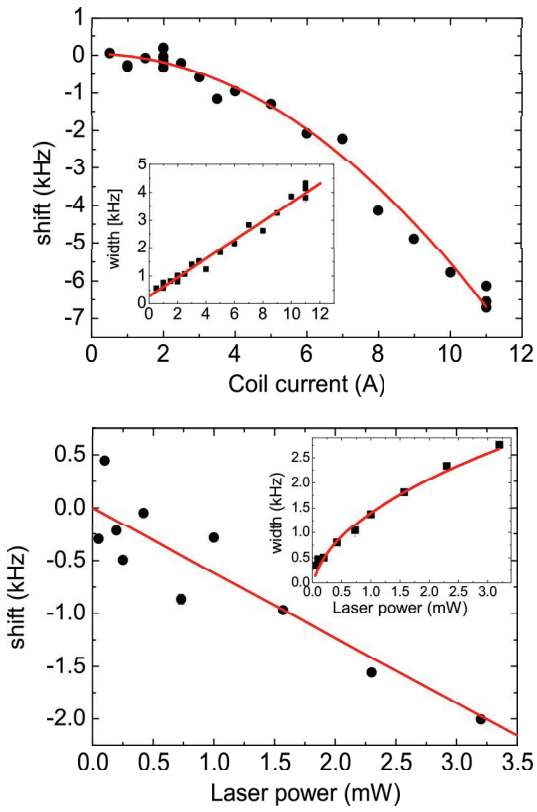

Fig. 4. Measurement of second order Zeeman shift (upper graph) and probe light shift (lower graph) for the 698 nm clock transition in a ^{88}Sr optical lattice clock. In the inset are reported the experimental FWHM of the observed transition. The experimental model agrees well with the theoretical expectation both for the shift and the width of the transition.

T = 1.5 μK.

In one sense, this effect has the obvious benefit of making the transition easy to find, even in the presence of reasonably large shot-to-shot atom number fluctuations. Thus overdriving the transition is now a standard part of our search algorithm. However, this effect could also present a strong limitation for operating a ^{88}Sr 1D lattice clock at high densities, and underfilled 2D traps or 3D traps could be the only way to overcome this effect in view of making an accurate optical lattice clock based on bosonic ^{88}Sr.

V. Systematics evaluation

A preliminary study of the systematics in our clock has been carried out by using an interleaved scheme and using the ULE cavity for the stabilzation of the clock laser as a frequency reference. The value for the shift and the width of the clock transition are reported in fig.4 for different values of coil current (used to produce the static magnetic field) and probe power.

Values of expected systematic shifts on the $^1S_0 \leftrightarrow {}^3P_0$ clock transition are reported in table I. Values are calculated

TABLE I

Evaluation of systematic shift of 1S0-3P0 clock transition for ^{88}Sr in typical conditions (see text for details).

Effect	Shift (Hz)	Uncertainty (Hz)
1^{st} order lattice	-	1.5
2^{nd} order Zeeman	-20.4	10.1
probe AC Stark	-93	250
Blackbody radiation	2.2	0.1
Total uncertainty		252 Hz

for typical experimental condition for spectroscopy with an applied static magnetic field of B=1.3(0.3) mT, probe power P=150(50) μW, and chamber temperature of T=293(3) K.

At present the estimated uncertainty is limited to about 250 Hz by the uncertainty in the determination of probe light shift determined by the fit of data in fig.4. More accurate measurement of this effect would reduce further the overall uncertainty.

VI. Summary

As lattice clocks (and optical clocks in general) continue to improve, it is also important that we continue to look for ways to simplify the clocks, so they can reach a wider range of applications. We have now demonstrated several key facets of an ultimately transportable lattice clock system. We have constructed an apparatus that uses only lasers based on semiconductor technology, which greatly reduces the size and power requirements over previous versions. We have also shown how the comparatively small ^{3}P fine structure splitting in Sr allows us to quickly find the clock transition without relying on extensive metrology apparatus. In thes course of this development, we found a way to achieve extremely high levels of ground-state population depletion (more than 99 %), which further expedites the search procedure. An initial investigation into the source of the unexpectedly high contrast revealed evidence of density dependent collisions, an effect we plan to explore in more detail in future studies.

Acknowledgements We thank G. Ferrari, A. Alberti, V. Ivanov, R. Drullinger, F. Sorrentino and M. Bober for their work in the initial part of the experiment. We thank S. Chepurov, D. Sutyrin, and U. Sterr for helpful discussions and S. Xiao and R. Fox for a careful reading of the manuscript. We thank INOA staff for the loaning of wavelength meter used in this work. This work was supported by LENS under contract RII3 CT 2003 506350, Ente CRF, ASI, and ESA.

References

[1] T. Rosenband, D.B. Hume, P.O. Schmidt, C.W. Chou, A. Brusch, L. Lorini, W.H. Oskay, R.E. Drullinger, T.M. Fortier, J.E. Stalnaker, S.A. Diddams, W.C. Swann, N.R. Newbury, W.M. Itano, D.J. Wineland, and J.C. Bergquist , Science **319**, 1808 (2008)

[2] S. Blatt, A. D. Ludlow, G. K. Campbell, J. W. Thomsen, T. Zelevinsky, M. M. Boyd, and J. Ye, X. Baillard, M. Fouch, R. Le Targat, A. Brusch, and P. Lemonde, M. Takamoto, F.-L. Hong, and H. Katori, V. V. Flambaum, Phys. Rev. Lett. **100**, 140801 (2008)

[3] D. Kleppner, Phys. Today **59** , 10 (2006)

[4] G. Ferrari, P. Cancio, R. Drullinger, G. Giusfredi, N. Poli, M. Prevedelli, C. Toninelli, and G. M. Tino, Phys. Rev. Lett. **91**, 243002 (2003)

[5] M. Takamoto, F.-L. Hong, R. Higashi, and H. Katori, Nature (London) **435**, 321 (2005).
[6] A. D. Ludlow, T. Zelevinsky, G. K. Campbell, S. Blatt, M. M. Boyd, M. H. G. de Miranda, M. J. Martin, J. W. Thomsen, S. M. Foreman, Jun Ye, T. M. Fortier, J. E. Stalnaker, S. A. Diddams, Y. Le Coq, Z. W. Barber, N. Poli, N. D. Lemke, K. M. Beck, C. W. Oates, Science **319**, 1805 (2008)
[7] N. Poli, M. G. Tarallo, M. Schioppo, C. W. Oates and G. M. Tino, in press on Appl. Phys. B (2009)
[8] X. Baillard, M. Fouché, R. Le Targat, P. G. Westergaard, A.Lecallier, F. Chapelet, M. Abgrall, G. D. Rovera, P. Laurent, P. Rosenbusch, S. Bize, G. Santarelli, A. Clairon, P. Lemonde, G. Grosche, B. Lipphardt, and H. Schnatz, Eur. Phys. Jour. D **48**, 11 (2008).
[9] T. Legero, J.S.R. Winfred, F. Riehle, U. Sterr, IEEE proceedings of EFTF-FCS, 119 (2007) DOI: 10.1109/FREQ.2007.4319045
[10] A.V. Taichenachev, V.I. Yudin, C.W. Oates, C.W. Hoyt, Z.W. Barber, and L. Hollberg, Phys. Rev. Lett. **96**, 083001 (2006).
[11] X. Baillard, M. Fouch, R. L. Targat, P. G. Westergaard, A. Lecallier, Y. L. Coq, G. D. Rovera, S. Bize, and P. Lemonde, Opt. Lett. **32**, 1812 (2007).
[12] N. Poli, Z. W. Barber, N. D. Lemke, C. W. Oates, L. S. Ma, J. E. Stalnaker, T. M. Fortier, S. A. Diddams, L. Hollberg, J. C. Bergquist, A. Brusch, S. Jefferts, T. Heavner, and T. Parker, Phys. Rev. A **77**, 050501 (2008)
[13] N. Poli, R. E. Drullinger, G. Ferrari, M. Prevedelli, F. Sorrentino, M. G. Tarallo, and G. M. Tino, Proc. SPIE **6673**, 66730F (2007) DOI:10.1117/12.739057
[14] N. Poli, R. E. Drullinger, M. G. Tarallo, and G. M. Tino, IEEE proceedings of EFTF-FCS, 655, (2007) DOI:10.1109/FREQ.2007.4319155
[15] A. D. Ludlow, X. Huang, M. Notcutt, T. Zanon-Willette, S. M. Foreman, M. M. Boyd, S. Blatt, J. Ye, Opt. Lett. **32**, 641 (2007)
[16] M. G. Tarallo, Ph.D. Thesis, Universita' di Pisa (2009), unpublished. Available at http://coldatoms.lens.unifi.it/optical-atomic-clock/documents.html
[17] M. M. Boyd, A. D. Ludlow, S. Blatt, S. M. Foreman, T. Ido, T. Zelevinsky, and J. Ye, Phys. Rev. Lett. **98**, 083002 (2007).
[18] T. Ido, T. H. Loftus, M. M. Boyd, A. D. Ludlow, K. W. Holman, and J. Ye Phys. Rev Lett **94**, 153001 (2005)
[19] G.M. Tino, M. Barsanti, M. Angelis, L. Gianfrani and M. Inguscio, Appl. Phys. B **55**, 397 (1994)
[20] H. P. Layer, R. D. Deslattes, and W. G. Schweitzer, Jr., Appl. Opt. **15**, 734 (1976)
[21] P. Bohlouli-Zanjani, K. Afrousheh, and J. D. D. Martin, Rev. Sci. Instrum. **77**, 093105 (2006)
[22] Similar set of equations have also been used in J. S. R. Vellore Winfred et al., Poster at 7^{th} Symposium of Frequency standards and Metrology, Asilomar CA (2008)
[23] A. Traverso et al., arXiv:0809.0936 (2008)